Supporting Information

Effect of Singlet Oxygen on Redox Mediators in Lithium-Oxygen Batteries

Hyun-Wook Lee,[ab] Ja-Yeong Kim,[ab] Joo-Eun Kim,[b] Yun-Joo Jo,[b] Daniel Dewar,[c] Sixie Yang,[c] Xiangwen Gao,[c]* Peter G. Bruce[c]* and Won-Jin Kwak[ab]*

[a] School of Energy and Chemical Engineering, UNIST, Ulsan, 44919, Republic of Korea
[b] Department of Energy Systems Research, Ajou University, Suwon, 16499, Republic of Korea
[c] Department of Materials, University of Oxford, Oxford, U.K.
* Correspondence: xiangwen.gao@materials.ox.ac.uk; peter.bruce@materials.ox.ac.uk; wjkwak@unist.ac.kr

Experimental

Materials. *N,N,N′,N′*-tetramethyl-p-phenylenediamine (TMPD, 99 %, Sigma Aldrich), tetrathiafulvalene (TTF, 99 %, Tokyo chemical Inc.), 2,2,6,6,-tetramethylpiperidine-1-oxyl (TEMPO, 98 %, Alfa Aesar), tris[4-(diethylamino)phenyl]amine (TDPA, 99 %, Sigma Aldrich), 10-methylphenothiazine (MPT, 98 %, Alfa Aesar), 9,10-dimethylanthracene (DMA, Sigma Aldrich) and *meso*-tetraphenylporphine (TPP, Alfa Aesar) were stored in Ar filled glove box and used as purchased. Tetraethylene glycol dimethyl ether (TEGDME, 99 %, Acros Organics) was dried for 3 days with activated molecular sieve before used. Nafion D520 (5 wt. % in mixture of lower aliphatic alcohols and water, contains 45 % water, Sigma Aldrich), LiOH•H_2O (Samchun), dimethyl sulfoxide (DMSO, 99.9 %, Sigma Aldrich), α-Al_2O_3 (250 -450 nm, Alfa Aesar), Li_2O_2 powder (95 %, Alfa Aesar), dimethyl sulfoxide-d_6 (DMSO-d_6, 99.5 %, D, 99.9 %, Cambridge Isotope Laboratories, Inc), 2-tert-butyl-1,4-benzoquinone (BQ, > 98 %, Tokyo chemical Inc.) and acetonitrile (ACN, 99.9 %, Samchun) were used without any further treatment**.** Lithium metal foils were purchased from Honjo Metal and kept in Ar filled glove box. Gas diffusion layers (GDL, Sigracet 39 BB, Fuel Cell Store), glass fibers (GF/C, Whatman) and lithium bis(trifluoromethanesulfonyl)imide (LiTFSI, 99 %, Samchun) were dried over vacuum oven for 3 days at 120 ℃ before used.

Electrochemical measurement. Electrochemical experiments were conducted through galvanostat/potentiostat (WBSCS 3000Ls, WonATech, Korea) under 25 ℃. For cyclic voltammetry tests, platinum wire, glassy carbon (3 mm) and RE-7 (0.01 M Ag/Ag$^+$ in acetonitrile) were used as counter, working and reference electrode, respectively. All Li foils were coated with protective layer following previously reported method.[q] Electrolyte consists of 1 M LiTFSI, 50 mM additives and 0.5 mM TPP in TEGDME and was used 100 ul. The Li_2O_2 decomposition kinetic of RMs was measured at 10 mV s^{-1} of scan rate with rotating ring disk electrode (RRDE-3A, ALS) adapting same configuration applied for cyclic voltammetries but at 250 rpm of rotating speed. Solutions for RRDE test contained 1 M LiTFSI, 1 mM additive and 0.01 mM TPP in TEGDME. 30 mM of Li_2O_2 powder was sonicated for 5 minutes after added into each solution when kinetic of Li_2O_2 decomposition was measured.

UV-Vis and nuclear magnetic resonance (NMR) analysis. UV-Vis absorption spectra were obtained by Optizen POP UV-Vis spectrophotometer (KLAB). Detection of $^1O_2$ evolution during cycle was conducted with electrolyte containing 30 mM of DMA and was diluted into 37.5 ml of TEGDME after discharging to give adequate absorbance. In observation of reactivity, all solutions consist of 1 M LiTFSI, 50 mM additives and 0.5 mM TPP and were exposed to light source which has maximum wavelength at 525 nm (525PF, HepatoChem) over set time. Before measuring spectrum, each solution

was diluted into 1/1000 scale to exhibit proper intensity and ACN was used as diluent due to the high UV cut-off of TEGDME. (Solution with TDPA was diluted into 1/2000 scale since TDPA has much higher absorbance.) Scavenging ability of RMs and RM^{exp}s were obtained with solution containing 1 M LiTFSI, 30 uM additives, 0.3 uM TPP and 80 uM DMA, and same light source stated above was used. For TDPA and TTF, spectra of each time period were normalized after measurement since both have spectra affecting to spectrum of DMA. Samples of each RM and RM^{exp} were dissolved in DMSO-d$_6$ and ^{1}H NMR tests with 850 MHz Cryo NMR spectrometer (AVNACE III HD, Bruker, Germany).

Supplementary Discussion

Discussion 1. The suitability of DMA as a prove of $^1O_2$ in charging

DMA is possibly not a suitable probe during charging since DMA itself begins oxidation at just under 4.0 V (vs Li^+/Li), which is commonly in the charging potential range of LOBs. (Fig. S2) The $^1O_2$ evolution rate differs depending on the tool used for measurement. The highest $^1O_2$ yield during charging is 27 %, which is measured by home-made in-situ UV-Vis spectroscopy. However, this value was acquired using DMA, so we note that this number may be overestimated due to the instability of DMA at high potentials. Simultaneously, this number may also be underestimated since DMA is in competition with other cell components that may react with $^1O_2$. Therefore, we cannot measure the exact evolution rate of $^1O_2$ in charging, but only in discharging.

Discussion 2. The effect of TPP in chemical and electrochemical measurement

The UV-Vis spectrum of TPP remained unchanged within 48 hours of illumination and its CV showed no recognizable redox peaks because of its low concentration. This confirmed the suitability of TPP as a means to generate $^1O_2$ without showing changes to the measurements unrelated to the RM chemistry (Fig. S4). The stability of RMs with the presence of TPP was examined by recording the UV-Vis spectra of each RM without illumination. (Fig. S5) The intensity of TPP was sustained in all systems while the spectrum of each RM showed some changes indicating self-degradation of RMs within 48 hours of rest. However, comparing the spectra with illumination shown in Fig. 1 and S3, the effect of self-degradation was much smaller than the effect of $^1O_2$ on the degradation of RMs. Therefore, RMs degradation observed via UV-Vis in Fig.1 and S3 are mainly resulted from the reaction of $^1O_2$ with RMs in solution.
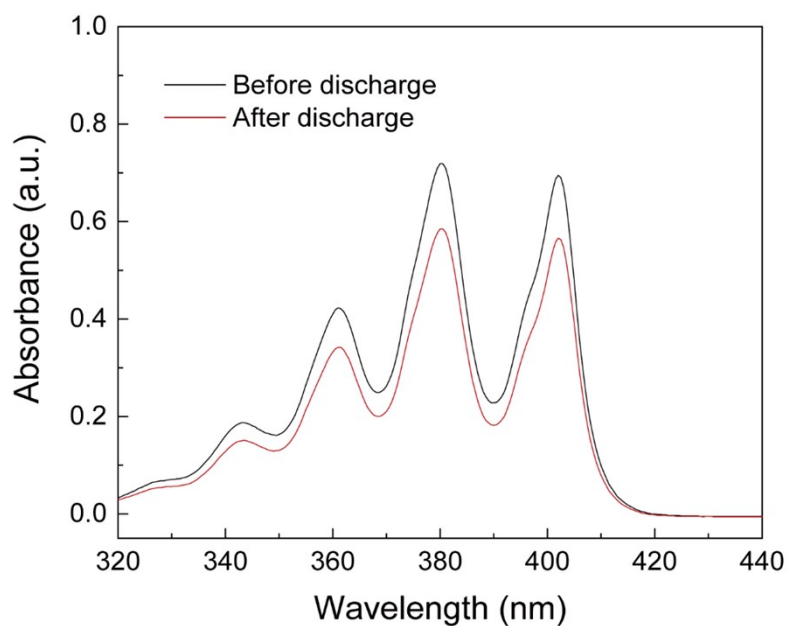
Supplementary Figures

Figure S1. $^1O_2$ evolution after discharge. Absorption spectra of electrolyte containing 30 mM of DMA before and after discharged at 0.1 mA cm^{-2} in the limited capacity of 0.5 mA cm^{-2}. Decreased absorbance indicates amount of $^1O_2$ evolved during discharge.
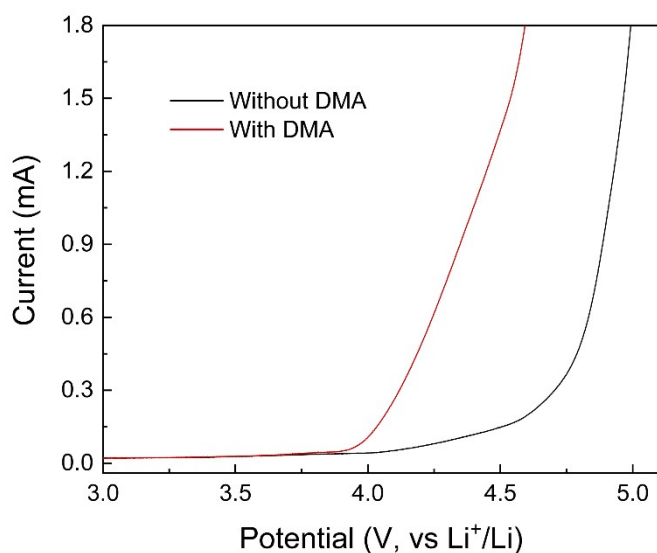

Figure S2. Linear sweep voltammetry (LSV) results of electrolyte only with DMA. 1 M LiTFSI, 30 mM DMA in TEGDME was used with Li metal up to 5.0 V at 1 mV s^{-1}.
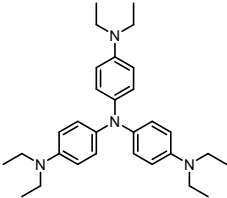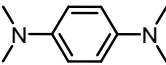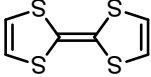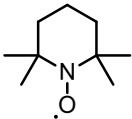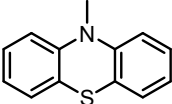
Redox mediator	Chemical structure	Current density	Capacity limit	Maximum cycle number
TDPA[1]		0.1 mA cm^{-2}	0.4 - 0.6 mAh cm^{-2}	100
TMPD[2]		500 mA g^{-1}	1000 mAh g^{-1}	50
TTF[3]		0.078 - 1 mAh cm^{-2}	0.045 - 1.5 mAh cm^{-2}	100
TEMPO[4]		0.1 mAh cm^{-2}	500 mAh g^{-1} (0.1910 - 0.3183 mAh cm^{-2})	50
MPT[5]		150 mA g^{-1}	1000 mAh g^{-1}	50

Table S1. Cyclability of RMs measured in the literatures. The summarized cyclability of RMs investigated in this work. Typically, RMs in LOBs exhibited low charging potential for 50 cycles, and sometimes 100 cycles have been reported. Thereby, the total amount of $^1O_2$ evolved is proportional with cycle numbers.
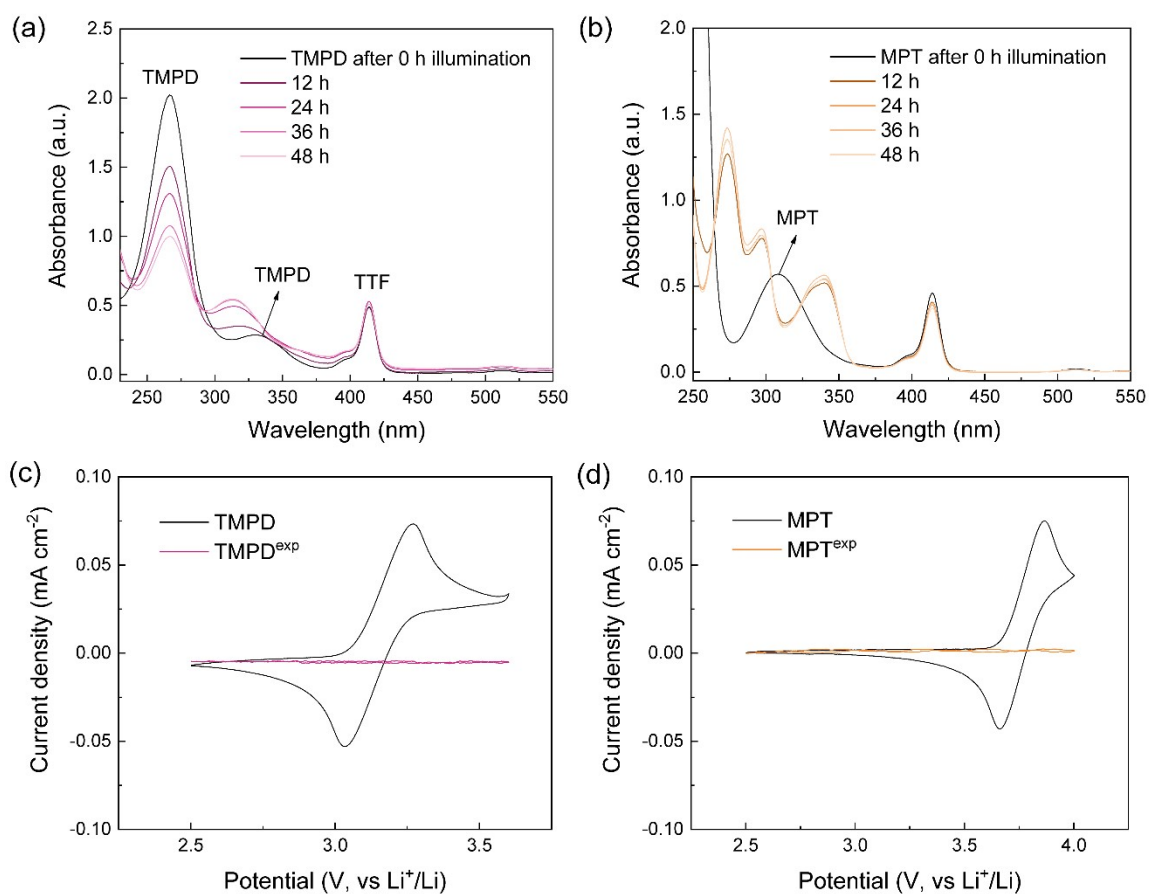
Figure S3. Reactivity with $^1O_2$ and electrochemical redox sustainability of RMs. UV-Vis spectra of (a) TMPD and (b) MPT for every 12 hours. Each samples were diluted with ACN into 50 uM RM and 0.5 uM TPP. Cyclic voltammetry of (c) TMPD and (d) MPT before and after 48 hours of illumination scanned at 1 mV s^{-1} using 50 mM RM in TEGDME with 0.5 mM TPP under Ar atmosphere.
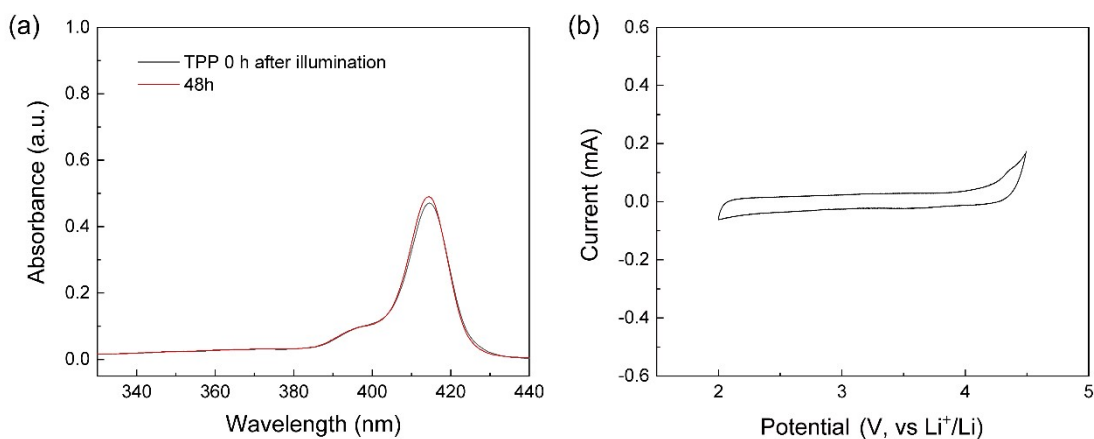
Figure S4. Reactivity of TPP towards $^1O_2$ and redox reaction. (a) UV-Vis spectra of TPP before and after 48 hours of illumination for $^1O_2$ evolution. 1M LiTFSI, 0.5 mM TPP was diluted in to 1/1000 scale with ACN. (b) Cyclic voltammetry (CV) of TPP using 1M LiTFSI, 0.5 mM TPP in TEGDME. CV conducted at 1 mV s^{-1} and potential range of 2 - 4.5 V. Increased current starting from 4.2 V indicates decomposition of TEGDME.
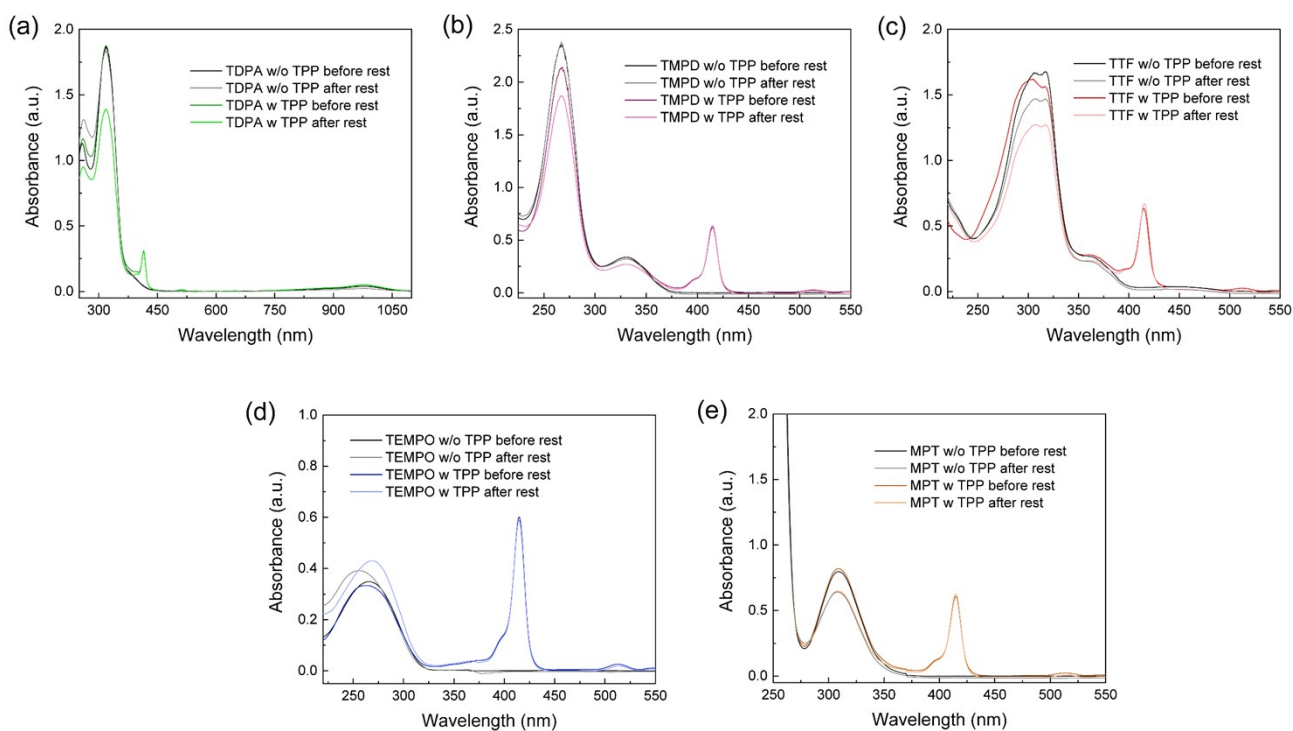

Figure S5. Stability of redox mediators contact with TPP. UV-Vis spectra of 50 uM (a) TDPA, (b) TMPD, (c) TTF, (d) TEMPO and (e) MPT with or without the presence of 0.5 uM of TPP, and without illumination for 48 hours. The intensity of TPP near 420 nm was barely change but on the other hand, RMs spectrum were change after rest indicating self-degradation along with time.
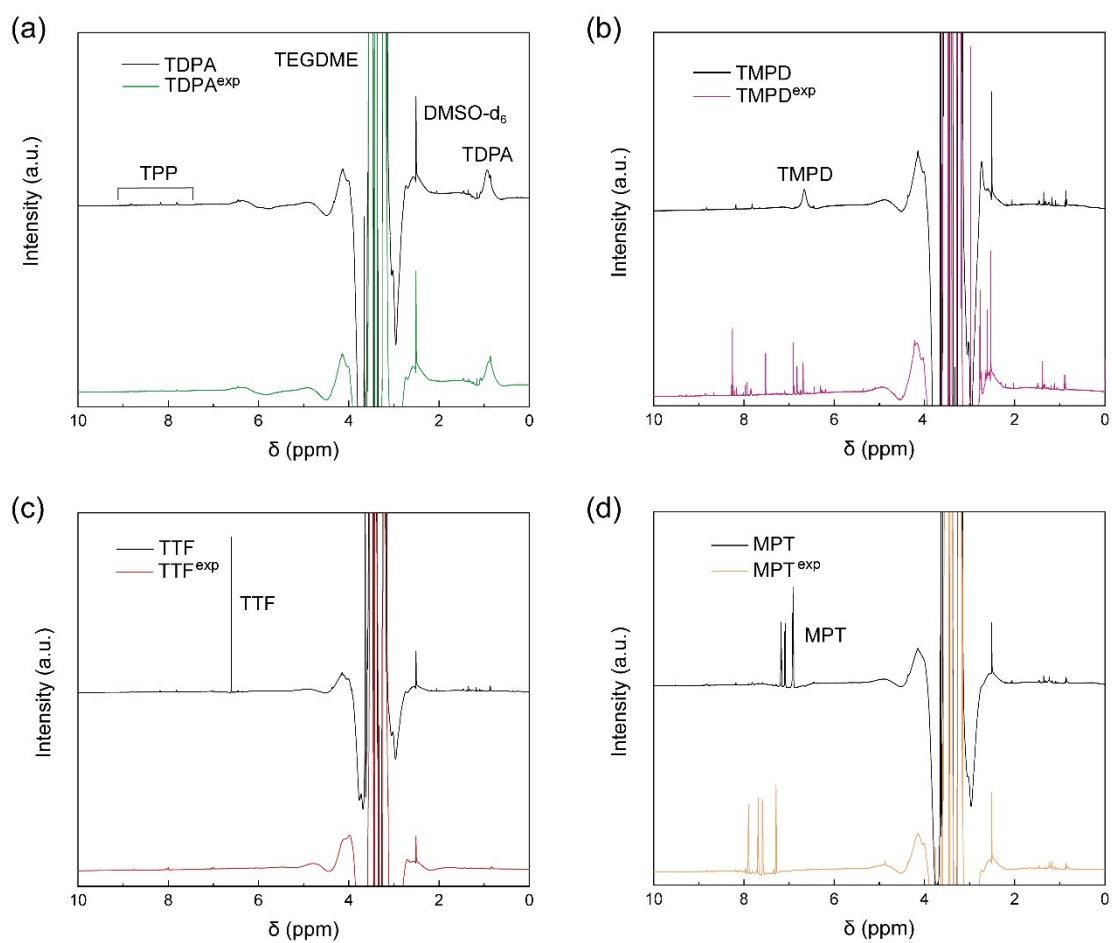
Figure S6. Nuclear magnetic resonance spectra of RMs. (a) TDPA, (b) TMPD, (c) TTF and (d) MPT before and after 48 hours of $^1O_2$ exposure. Peak commonly appeared near 2.5 ppm indicates DMSO-d_6 used as solvent for NMR.
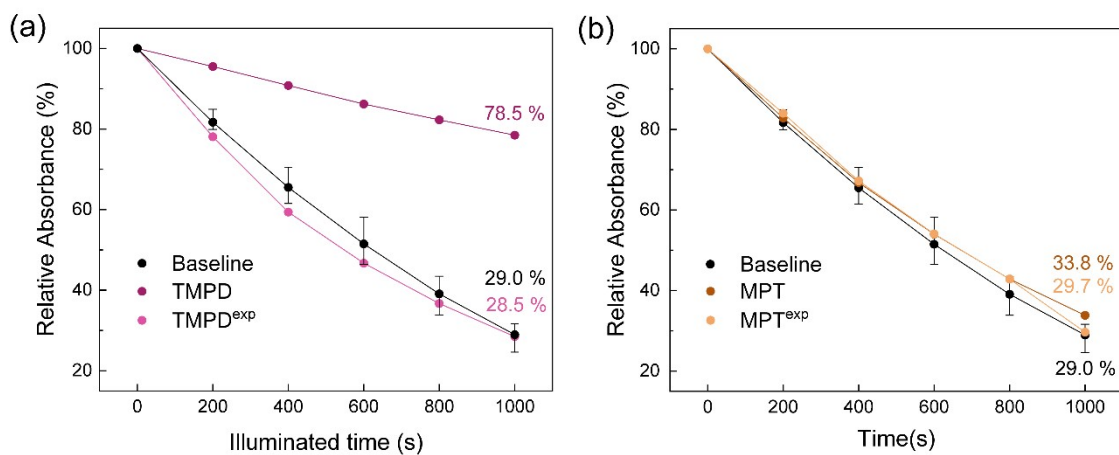
Figure S7. $^1O_2$ scavenging efficiency of RM and RM^{exp}. Relative absorbance of DMA for 1000 s exposed to $^1O_2$ evolved by 0.3 uM of TPP with the presence of 30 uM of (a) TMPD and TMPD^{exp} and (b) MPT and MPT^{exp} in TEGDME. 80 uM of DMA was used in initial solution stirred at 150 rpm and O_2 was purged with rate of 1 ml min^{-1}. Absorbance of DMA was measured at 379.5 nm via UV-Vis spectrometer.

Redox mediator	Initial absorbance of DMA with RM (a.u.)	Absorbance of DMA after 1000 s with RM (a.u.)	Normalized Absorbance of DMA after 1000 s with RM (%)	Absorbance of DMA after 1000 s in baseline (%)	Scavenging rate (%)
TDPA	0.83	0.44	52.11	28.98	32.55
TDPA^{exp}	0.89	0.40	45.32	28.98	23.00
TMPD	0.92	0.73	78.48	28.98	69.73
TMPD^{exp}	1.01	0.36	28.48	28.98	-0.68
TTF	0.66	0.24	35.60	28.98	9.32
TTF^{exp}	0.67	0.20	29.32	28.98	0.45
TEMPO	0.94	0.26	27.87	28.98	-1.52
TEMPO^{exp}	0.92	0.29	31.15	28.98	3.13
MPT	0.80	0.27	33.83	28.98	6.79
MPT^{exp}	0.78	0.23	29.68	28.98	1.01

Table S2. Data sheet used for calculating scavenging rate of RMs and RM^{exp}s. Each RMs scavenging rate was calculated with DMA absorbance before and after exposure to $^1O_2$. Since certain RM has own absorption spectrum affecting to DMAs, absorbance was normalized when scavenging rate was calculated and scavenging rate is calculated following equation.

$$Scavenging\ rate\ (\%) = \frac{Abs_{rel,\ additive}\ (\%) - Abs_{rel,\ baseline}\ (\%)}{100 - Abs_{rel,\ baseline}\ (\%)} * 100\ \%$$
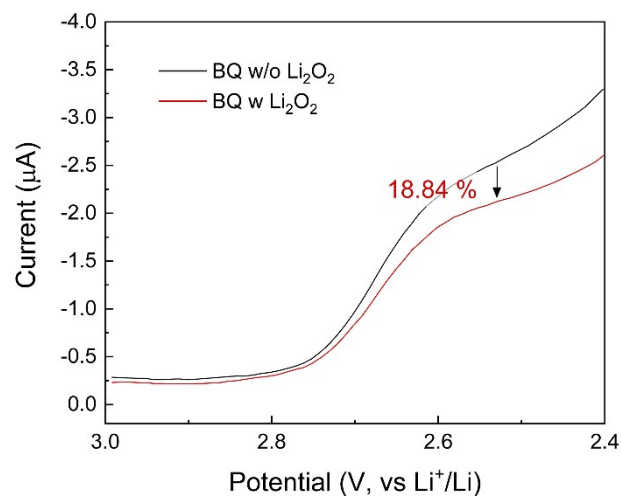
Figure S8. Measurement of difference in viscosity by Li$_2$O$_2$. LSV curves of 1 mM 2-tert-butyl-1,4-benzoquinone (BQ) at 10 mV s^{-1}, 250 rpm. Electrolyte consists of 1 M LiTFSI, 0.01 mM TTP and with or without 30 mM Li$_2$O$_2$.
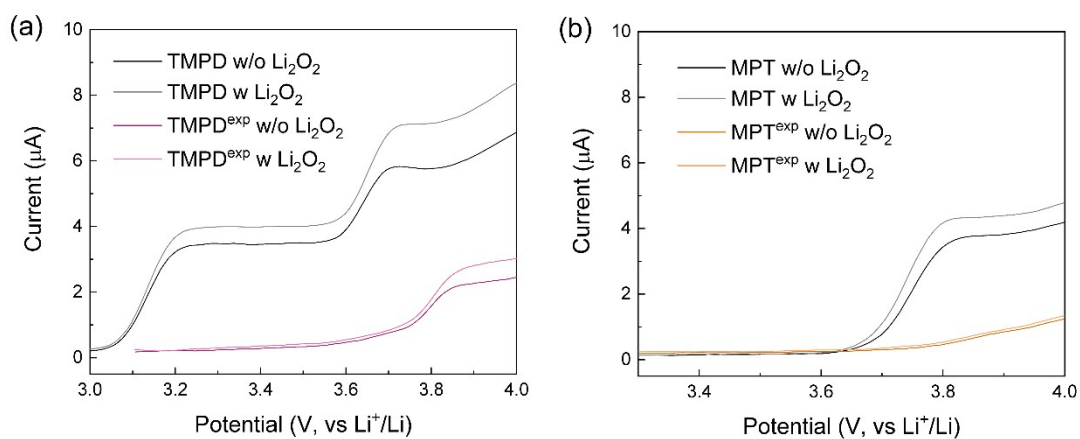

Figure S9. Oxidation kinetics of RMs towards Li$_2$O$_2$. LSV curves of 1 mM (a) TMPD and TMPD[exp], and (b) MPT and MPT[exp] at 10 mV s^{-1}, 250 rpm, respectively. Electrolyte consisted of 1 M LiTFSI, 0.01 mM TTP and with or without 30 mM Li$_2$O$_2$.

References

1   D. Kundu, R. Black, B. Adams and L. F. Nazar, *ACS Cent. Sci.*, 2015, **1**, 510–515.

2   C. Zhang, N. Dandu, S. Rastegar, S. N. Misal, Z. Hemmat, A. T. Ngo, L. A. Curtiss and A. Salehi-Khojin, *Adv. Energy Mater.*, 2020, **10**, 2000201.

3   Y. Chen, S. A. Freunberger, Z. Peng, O. Fontaine and P. G. Bruce, *Nat. Chem.*, 2013, **5**, 489–494.

4   B. J. Bergner, A. Schürmann, K. Peppler, A. Garsuch and J. Janek, *J. Am. Chem. Soc.*, 2014, **136**, 15054–15064.

5   N. Feng, X. Mu, X. Zhang, P. He and H. Zhou, *ACS Appl. Mater. Interfaces*, 2017, **9**, 3733–3739.